Nanodiamonds and wildfire evidence in the Usselo horizon postdate the Allerød-Younger Dryas boundary

Annelies van Hoesel[a,b,1], Wim Z. Hoek[b], Freek Braadbaart[a,c], Johannes van der Plicht[d,e], Gillian M. Pennock[a], and Martyn R. Drury[a]

[a]Department of Earth Sciences, Budapestlaan 4, 3584 CD, Utrecht, The Netherlands; [b]Department of Physical Geography, Utrecht University, Heidelberglaan 2, 3584 CS, Utrecht, The Netherlands; [c]Institute of Biology, Leiden University, PO Box 9505, 2300 RA, Leiden, The Netherlands; [d]Center for Isotope Research, Groningen University, Nijenborgh 4, 9747 AG, Groningen, The Netherlands; and [e]Faculty of Archaeology, Leiden University, Reuvensplaats 3, 2311 BE, Leiden, The Netherlands

Edited by Mark H. Thiemens, University of California at San Diego, La Jolla, CA, and approved March 23, 2012 (received for review December 23, 2011)

The controversial Younger Dryas impact hypothesis suggests that at the onset of the Younger Dryas an extraterrestrial impact over North America caused a global catastrophe. The main evidence for this impact—after the other markers proved to be neither reproducible nor consistent with an impact—is the alleged occurrence of several nanodiamond polymorphs, including the proposed presence of lonsdaleite, a shock polymorph of diamond. We examined the Usselo soil horizon at Geldrop-Aalsterhut (The Netherlands), which formed during the Allerød/Early Younger Dryas and would have captured such impact material. Our accelerator mass spectrometry radiocarbon dates of 14 individual charcoal particles are internally consistent and show that wildfires occurred well after the proposed impact. In addition we present evidence for the occurrence of cubic diamond in glass-like carbon. No lonsdaleite was found. The relation of the cubic nanodiamonds to glass-like carbon, which is produced during wildfires, suggests that these nanodiamonds might have formed after, rather than at the onset of, the Younger Dryas. Our analysis thus provides no support for the Younger Dryas impact hypothesis.

radiocarbon dating | carbon spherules | wildfire temperature | electron microscopy

The exact cause of the onset of the Younger Dryas (YD) stadial (dated to approximately 12.9 ka) is still debated (1). Firestone et al. (2) proposed that an extraterrestrial impact over the North American ice sheet was not only the cause of the rapid cooling, but also resulted in worldwide high temperature biomass burning, North American megafaunal extinction, and the disappearance of the human Clovis culture. Evidence for this hypothesis has been under severe scrutiny ever since; most lines of evidence have proven to be not reproducible or not unique to an impact (see ref. 3 for an overview).

One of the more promising lines of evidence for the impact hypothesis is the alleged occurrence of nanodiamonds in Allerød-YD boundary sediments. At first, nanodiamonds were reported based on NMR analysis of so-called "glass-like" carbon—black, carbon-rich objects with an irregular shape and smooth reflective "glassy" surfaces (2). The peak in the NMR spectrum, however, might have been wrongly identified as diamond (4). More convincing evidence of nanodiamonds was subsequently reported by Kennett et al. (5, 6). Using transmission electron microscopy (TEM), they claim to have found several nanodiamond polymorphs in so-called carbon spherules—black, carbon-rich spherical objects with a honeycomb-like or open interior structure—and in bulk samples from the Black Mat, a marker horizon in North America dated to the Allerød-YD boundary. The polymorphs they reported include cubic (3C) diamond, lonsdaleite (2H diamond), and n-diamond (fcc carbon). Lonsdaleite is especially of interest because, in nature, it is reported only in meteorites (7) or in relation to impact craters (8, 9), and is generally formed through shock deformation of graphite or diamond. Lonsdaleite has, therefore, been previously taken as evidence for shock impact formation (9), although it can also be created in low quantities during carbon vapor deposition (CVD) (10, 11). Furthermore, the presence of lonsdaleite in impact craters has been challenged and the use of nanodiamonds as a diagnostic criterion for an impact is still debated (8, 9, 12, 13).

Daulton et al. (14), however, found no evidence of nanodiamonds in carbon spherules, glass-like carbon or microcharcoal aggregates from the Black Mat and other, non-Allerød-YD age, strata. Instead, they found graphene- and graphene/graphane-oxide aggregates in all their samples. Moreover, Daulton et al. (14) suggest that Kennett et al. (5, 6) did not find any nanodiamonds either but misinterpreted their diffraction data: mistaking graphene aggregates for cubic diamond and graphene/graphane aggregates for lonsdaleite. Later, the occurrence of n-diamond and lonsdaleite was also reported during a more extensive analysis on a layer of ice from the surface of the Greenland ice sheet (15). The layer of ice in which these nanodiamonds were found was indirectly dated to the onset of the YD, although Pinter et al. (3) suggest the oxygen isotope signal might have been misinterpreted and actually points to a Holocene age. In Europe, cubic nanodiamonds were found in the Usselo horizon at Lommel, Belgium (16). However, no age control was presented and no lonsdaleite or n-diamond was found. Recently, nanodiamonds similar to those found in Greenland were found in Mexican lake sediments thought to represent the Allerød-YD boundary (17). However, even if their age-depth model is correct, the 10-cm-wide peak in nanodiamonds might reflect 5,890 y of deposition (18). The occurrence and origin of nanodiamonds, and especially lonsdaleite, in the YD boundary sediments is thus still uncertain.

In the Northwestern European coversand area, the onset of the YD is often stratigraphically marked by the Usselo horizon, a buried/fossil soil horizon formed during the Allerød to early YD (19). During the second half of the YD, the Usselo horizon was covered by the Younger Coversand II (20). The Usselo horizon should thus have collected any impact material falling from the atmosphere during the Allerød to early YD. We investigated the Usselo horizon at Geldrop-Aalsterhut, The Netherlands (Fig. 1 and Fig. S1) for the occurrence of nanodiamonds using TEM. Bulk charcoal from the Usselo horizon at Geldrop has been previously dated (21) to $11{,}020 \pm 230$ ^{14}C B.P., 13,110–12,680 calibrated (cal.) y B.P. (sample GrN-603), and to $10{,}960 \pm 85$ ^{14}C B.P., or 12,935–12,695 cal. y B.P. (sample GrN-1059). These ^{14}C dates are from the early days of radiocarbon dating; they were measured by radiometry and are thus imprecise compared

Author contributions: W.Z.H. and M.R.D. designed research; A.v.H., W.Z.H., F.B., and J.v.d.P. performed research; A.v.H., W.Z.H., F.B., and J.v.d.P. analyzed data; and A.v.H. and G.M.P. wrote the paper.

The authors declare no conflict of interest.

This article is a PNAS Direct Submission.

[1]To whom correspondence should be addressed. E-mail: a.vanhoesel@uu.nl.

This article contains supporting information online at www.pnas.org/lookup/suppl/doi:10.1073/pnas.1120950109/-/DCSupplemental.

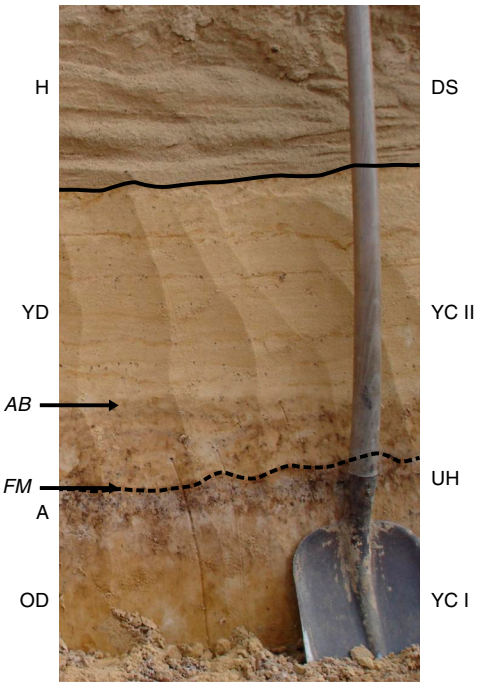

Fig. 1. The Late Glacial-Holocene stratigraphy at Geldrop-Aalsterhut. Approximate time periods are given on the left, stratigraphy on the right. From bottom to top: Aeolian deposits belong to the Younger Coversands I (YC I) formed during the Older Dryas (OD) cold stadial. The Usselo horizon (UH), which formed in the top of the YC I during the warmer Allerød (*A*) interstadial and into the early part of the Younger Dryas (YD) cold stadial, is visible as a bleached layer with charcoal particles. The Younger Coversands II (YC II) were subsequently deposited on top of the UH due to continued aeolian activity as vegetation cover diminished during the YD. There is an erosional boundary to the Holocene (H) driftsands (DS), which represent renewed aeolian activity due to human activity during the Middle Ages. The soil that had formed before Medieval times has been eroded at this location. Occupation horizons of the Federmesser (FM) and the Ahrensburg (AB) culture are indicated with arrows. The Ahrensburg occupation horizon at Geldrop has been dated within 10,600–9,800 ^{14}C y B.P. (24). The Federmesser culture had mostly disappeared from the Benelux near the end of the Younger Dryas (24–26). At Geldrop, their occupation horizon coincides with the Usselo horizon.

to modern standards, in particular sample GrN-603. Here we report on more precise accelerator mass spectrometry (AMS) dates for 14 individual charcoal particles, 12 from the Usselo horizon, and 2 from just above the horizon. In addition, the reflectance of several charcoal particles was measured using light microscopy to estimate the wildfire temperature (22, 23).

Results

The AMS radiocarbon dates of carefully selected and cleaned individual charcoal particles from the charcoal-rich top part of the Usselo horizon show no correlation with depth and range over 400 ^{14}C y (Table 1). The weighted average of the charcoal particles from the Usselo horizon is $10{,}870 \pm 15$ ^{14}C y B.P. (12,785–12,650 cal. y B.P.). Bayesian analysis (27), however, shows that the two particles found slightly above the horizon (AH21a,b) are part of the same population (Fig. S2); it is likely that they were distributed due to bioturbation. Including these two particles yields a slightly younger average of $10{,}845 \pm 15$ ^{14}C y B.P. (12,760–12,640 cal. y B.P.); this is two centuries younger than the Black Mat layers in which hexagonal diamonds have been found (6), which have an average age of $11{,}070 \pm 10$ ^{14}C y B.P. (13,080–12,915 cal. y B.P.) (6). With the exception of one or two outliers in each dataset, the datasets show almost no overlap (Fig. 2); these outliers all have high standard deviations. When compared to other radiocarbon dated sites reported to

Table 1. AMS radiocarbon dates of the individual charcoal particles from the charcoal-rich top layer of the Usselo horizon at Geldrop-Aalsterhut (individually calibrated to calendar years)

Sample name	Depth, cm	Sample nr. for AMS	^{14}C age B.P.	Cal. age B.P.
AH-21a	−5.0−−4.0	GrA-49570	10,735 ± 45	12,675–12,585
AH-21b	−5.0−−4.0	GrA-49521	10,765 ± 50	12,700–12,595
AH-12a	0.0–2.0	GrA-49516	10,765 ± 50	12,700–12,595
AH-12b	0.0–2.0	GrA-49507	10,920 ± 50	12,870–12,695
AH-32a	0.0–2.0	GrA-49527	10,960 ± 60	12,915–12,715
AH-32b	0.0–2.0	GrA-49529	10,755 ± 55	12,695–12,590
AH-23a	0.0–2.0	GrA-49573	10,860 ± 45	12,795–12,640
AH-23b	0.0–2.0	GrA-49574	10,845 ± 45	12,775–12,630
AH-13a	2.0–4.0	GrA-49569	10,895 ± 45	12,840–12,670
AH-13b	2.0–4.0	GrA-49514	10,880 ± 110	12,880–12,640
AH-33a	2.0–4.5	GrA-49575	10,900 ± 50	12,850–12,675
AH-14a	4.0–5.5	GrA-49515	11,020 ± 75	13,065–12,775
AH-14b	4.0–5.5	GrA-49509	10,865 ± 55	12,810–12,640
AH-14c	4.0–5.5	GrA-49524	10,840 ± 75	12,795–12,615

The larger measurement errors are caused by the fact that the samples were very small, even for AMS. Samples were taken from different depth Usselo at three different locations (see Fig. S1). The depth of the samples is indicated using the top of the Usselo horizon as a reference level (0 cm). See Fig. S2 for a visual overview of the modeled and individually calibrated dates.

contain nanodiamonds (5), our layer is of similar age as Murray Springs (28) but older then Lake Hind (2).

Charcoal particles from the Usselo horizon show a reflectance of $0.96 \pm 0.06\%$ R_o, indicating a charring temperature of approximately 420 ± 10 °C, assuming a charring period of 1 h (22). This temperature is consistent with the occurrence of carbon spherules and glass-like carbon found within the horizon (Fig. 3), which are both thought to form during low-temperature wildfires (29, 30). Glass-like carbon (up to 150 particles/100 g) is more common in the Usselo horizon than carbon spherules (<10 particles/100 g). Charcoal is, however, the most abundant form of charred material (>10,000 particles/100 g). Although the charcoal particles, in most cases, have the characteristic cell structure of their precursor wood (Fig. 4*D*), the polished sec-

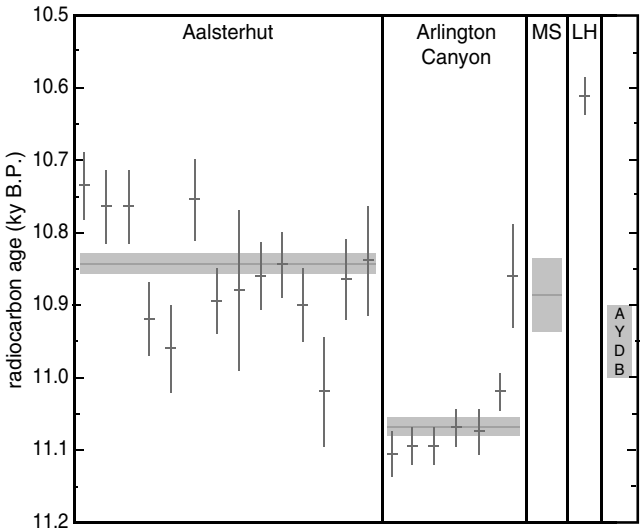

Fig. 2. Individual radiocarbon ages and weighted average (gray bands) of the charcoal particles from the Usselo horizon at Aalsterhut compared to those of the Black Mat at Arlington Canyon, where the alleged hexagonal diamonds have been found (6). The age of the lower boundary of the Black Mat at Murray Springs (MS, average of 8; ref. 28) and Lake Hind (LH, single date; ref. 2), where cubic and n-diamonds have been found (5) are also included. For reference, the approximate age of the Allerød-YD boundary (AYDB) is indicated (see *Discussion*).

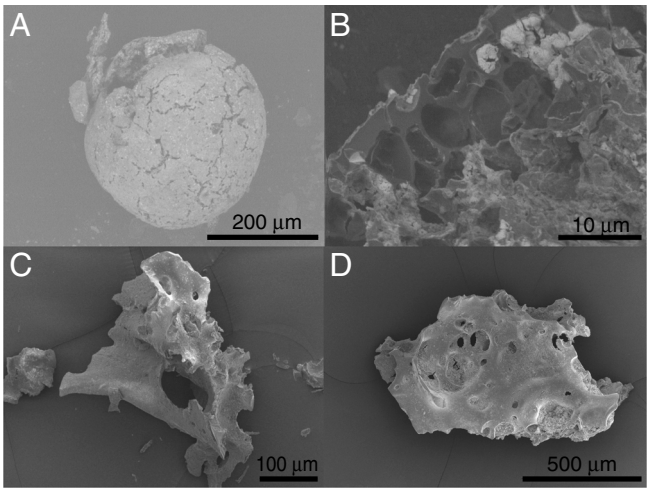

Fig. 3. Secondary electron SEM images of handpicked carbon spherules (sample AH-33) and glass-like carbon (sample AH-4). (*A*) Complete carbon spherule and (*B*) close-up of internal structure of a broken carbon spherule. Energy dispersive X-ray spectrometry shows that the spherules contain 45–90 wt % carbon; the other dominant element is oxygen. Although smaller (<0.3 mm in size compared to <2.5 mm in size), these particles look similar to the carbon spherules found in the Black Mat (2, 6), as well as to charred fungal sclerotia (29). (*C* and *D*) Examples of glass-like carbon showing smooth, glassy surfaces and irregular shapes. No remnant structure of the precursor wood, as in charcoal (Fig. 4 *A* and *B*), is visible.

tions also showed parts where no remnant cells were observed (Fig. 4*C*).

TEM analysis of crushed glass-like carbon particles shows the presence of carbonaceous microparticles similar to those interpreted by Kennet et al. (6) as lonsdaleite (Fig. 5 *A* and *C*). Diffraction rings containing discrete spots (Fig. 5 *B* and *D*), correspond to some of the known lonsdaleite spacings (7). The patterns, however, like the ones reported from the Black Mat (6), do not display rings associated with the unique 1.93 and 1.50 Å d spacings associated

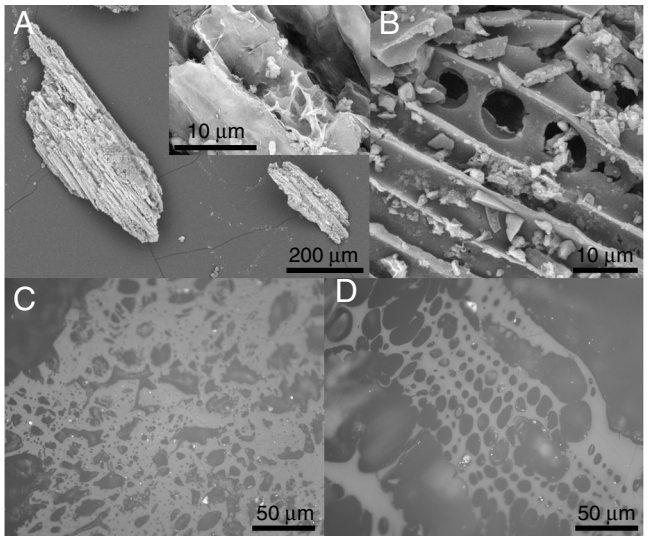

Fig. 4. Charcoal from the Usselo horizon. (*A*) Secondary electron (SE) image of two charcoal particles from the charcoal part of the Usselo horizon (sample AH-4) showing remnant structure from the cell walls of the precursor wood. The inset shows a higher magnification image of the particle on the left, showing detail of small-scale structure. (*B*) SE image of a different charcoal particle showing the same structure. (*C* and *D*) Reflective light image of two polished charcoal particles (sample AH-21) analyzed for their reflectance. The polished sample (*C*) shows no evidence of remnant cell walls, whereas, in *D*, cell walls are observed.

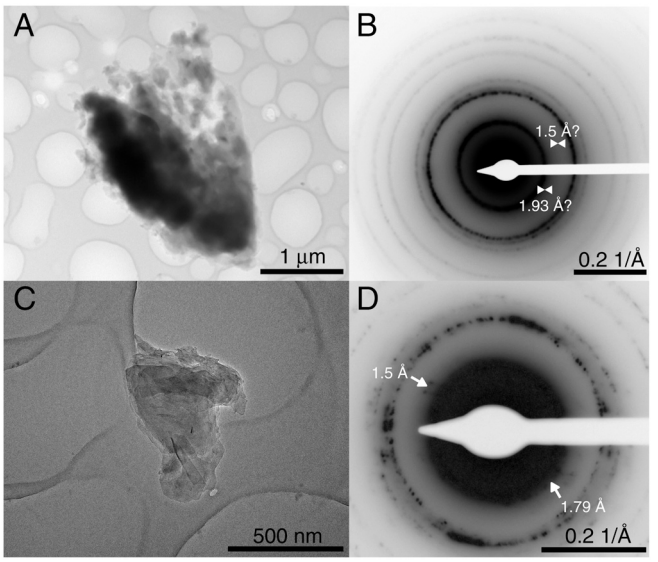

Fig. 5. Brightfield TEM images of carbonaceous microparticles within crushed glass-like carbon (*A* and *B*, sample AH-14; *C* and *D*, sample AH-33) and their associated diffraction patterns. Diffraction patterns are inverted for better visibility. (*B*) Diffraction pattern of (*A*) showing double diffraction rings corresponding to graphene/graphane aggregates, rather then lonsdaleite. The double triangles show the location of the missing 1.93 and 1.5 Å rings that should be present in the case of lonsdaleite. (*D*) Diffraction pattern of *C* showing discrete rings. The arrows indicate a few discrete spots corresponding to a d spacing of 1.5 and 1.79 Å, which are known spacings of graphite.

with lonsdaleite (7). The diffraction patterns of these particles are therefore more consistent with graphene–graphane aggregates instead (14). Some of the diffraction patterns (Fig. 5*D*) show a small number of grouped spots corresponding to the 1.54 and 1.79 Å d spacings of graphite and might therefore be closer to turbostratic carbon or disordered graphite than to the randomly stacked graphene/graphane aggregates.

Other, less common, polycrystalline particles show diffraction rings with d spacings corresponding to cubic diamond (Fig. 6), although the cubic diamond reflections are also close to those calculated for graphene (14). A 400 reflection however, which

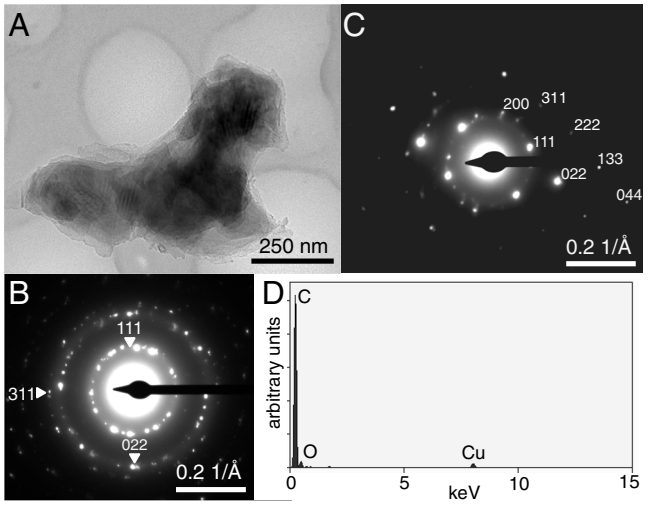

Fig. 6. (*A*) Brightfield TEM image of a polycrystalline diamond particle within crushed glass-like carbon from the lower part of the charcoal-rich layer (sample AH-14). (*B*) Diffraction pattern of the entire particle showing rings corresponding to the diamond d spacings and (*C*) [011] selected area diffraction pattern of a single diamond crystal from the particle in *A*. (*D*) The energy dispersive X-ray spectrum shows the carbonaceous nature of the particle, the small copper peak is from the copper grid used to support the holey carbon film.

has no equivalent in graphene, is weakly present. The selected area diffraction pattern of a small part of the particle (approximately 200 nm) in Fig. 6*A* yields a diffraction pattern (Fig. 6*C*) similar to the [011] pattern of cubic diamond (31). Weak 200 "forbidden" reflections, not forbidden for fcc carbon or n-diamond, are visible. They do not show up in the ring pattern and are, therefore, more likely the result of double diffraction within a cubic diamond crystal than an indicator for n-diamond.

Discussion

Wildfires. Our radiocarbon dates suggest that wildfires at this location occurred after the Allerød-YD transition. There are, however, uncertainties in the timing of the YD onset (1), as well as in the interpretation of wood-charcoal ages due to the "inbuilt age" effect (32). The inbuilt age occurs because consumption of the outer wood during a wildfire leaves charcoal with radiocarbon ages representing the older wood of the trees (32). In addition, many trees would have died as a result of wetter conditions during the early YD (33), possibly providing an older fuel source. Both these aspects of the inbuilt age result in the charcoal radiocarbon ages predating the wildfire event for an unknown number of years. The precise timing of the YD onset is still ambiguous (1) and the calibration curve for this interval is not definitive (34, 35). For Northwestern Europe the onset of the YD chronozone, which is marked by a change in vegetation, was originally defined at 11,000 ^{14}C y B.P. (36). This age corresponds to the increase in atmospheric ^{14}C starting between 11,000 and 10,950 ^{14}C y B.P., often referred to as the "radiocarbon cliff." This radiocarbon cliff is presumably related to the shutdown of the thermohaline circulation, and has been suggested as a global marker for the onset of the YD (1, 37–39). According to the current International Calibration 2009 (IntCal09) curve (34), the age of the radiocarbon cliff corresponds roughly to the onset of Greenland Stadial 1 at 12,850 y B.P. in the North Greenland Ice Core Project ice core (40). In The Netherlands, the clear shift in vegetation marked by an abrupt increase in nonarboreal pollen from numerous palynological records related to the onset of the YD occurred slightly later, around 10,950 ^{14}C y B.P. (41). An even younger age for the onset of 10,900 $\pm$ 50 ^{14}C y B.P. has been adopted when dating the North American Black Mats (28). Therefore, we use a range of 11,000–10,900 ^{14}C y B.P. for the Allerød-YD boundary (Fig. 2) in which the older half (11,000–10,950 ^{14}C y B.P.) corresponds best to the Northwestern European records (36, 39, 41). Within two standard deviations, our individual radiocarbon ages do not all overlap and show a gap of 45 ^{14}C y between the youngest and the oldest age (Table 1). This gap is within the lifespan of an individual pine tree, which can grow up to 200 y old, and less then the minimum fire frequency in present-day boreal forests of 50–200 y (42). When looking at the calibrated dates (Table 1), however, there is no gap, but an overlap of 35 cal. years within two standard deviations. Furthermore, when using Bayesian statistics (27), all ages overlap within one standard deviation (Fig. S2) and they are thus statistically the same.

The charcoal in the Usselo horizon at Geldrop-Aalsterhut can thus easily represent a single episode of wildfire, with the charcoal particles dispersed through the top of the Usselo horizon by bioturbation. In that case, taking into account the inbuilt age, all radiocarbon ages predate the actual wildfire and the maximum age of the youngest charcoal particle (AH-21a), 10,825 ^{14}C y B.P., provides a maximum age estimate of the timing of the wildfire (32). The wildfire thus occurred up to two centuries after the onset of the YD (Fig. 2). The wildfire is therefore not only low temperature, but also does not fall within the same time window as the proposed impact, which is contrary to suggestions by Firestone et al. (2). Moreover, when compared to the nanodiamond-bearing layer at Arlington Canyon (6), our wildfire is clearly younger (Fig. 2) and, therefore, must represent a different event. Our findings are, however, in agreement with several studies in North America showing the absence of evidence for continent-wide wildfires (43–45), let alone intercontinental wildfires reaching Europe.

Because our charcoal particles were derived from a soil horizon, which accumulates material over a long time period, it can also be argued that the dated charcoal particles represent multiple wildfires, rather then just one episode of biomass burning. Within the respective dating uncertainties, some of the older charcoal particles might then be related to a wildfire occurring around the onset of the YD; this does not, however, require a relation with the proposed impact, as frequent fires occurred naturally (42).

Origin of the Nanodiamonds. When considering the extraterrestrial impact hypothesis, there are several possibilities for the origin of the nano- and microdiamonds. They (*i*) originate from the impactor body, (*ii*) formed through shock-transformation processes during the impact, (*iii*) formed within the high temperature "fireball" resulting from the airburst or impact, (*iv*) could have arrived through continuous "meteoritic rain," or (*v*) formed through a terrestrial process unrelated to an impact.

i. Tian et al. (16) report that nanodiamonds found in the Usselo horizon at Lommel contained terrestrial isotopic δ^{13}C and C/N ratios, whereas Kurbatov et al. (15) note that the rounded n-diamonds they found in the Greenland ice sheet are "unlike any diamonds found in meteorites." These results suggest that these nanodiamonds did not originate from an impactor. In addition, a nanodiamond-bearing impactor would have been enriched in platinum group elements, which are absent in the YD boundary layer (46).
ii. The occurrence of lonsdaleite, although a rare but possible indicator of shock metamorphism, has not been independently confirmed. Lonsdaleite is, however, also absent in the K/T (Cretaceous/Tertiary) boundary, where only shock-produced cubic diamond was found (47). The morphology of the smaller (approximately 20 nm) nanodiamonds found by Tian et al. (16), however, suggest an isotropical growth mechanism for these diamonds rather than an anisotropic shock mechanism (11). In addition, no other shocked minerals have been reported from the Allerød-YD boundary.
iii. Isotropic growth is more consistent with CVD nanodiamond formation in the superheated fireball following an impact or airburst. The presence of carbon spherules and glass-like carbon in the YD boundary sediments, and in which nanodiamonds have been found, may, however, be inconsistent with such extreme temperatures, as current research suggests carbon spherules and glass-like carbon form at temperatures below 500 °C (29, 30). Furthermore, the larger (>100 nm) flake-like or tabular nano- and microdiamonds, found in the Black Mat as well as the Usselo horizon, cannot easily form by isotropic growth.
iv. Nanodiamonds have been found in micrometeorites and some interplanetary dust particles (48), which continuously rain down on Earth. However, these nanodiamonds are small (<5 nm) and thus do not explain the larger diamonds found in our work and elsewhere (6, 16). In addition, if the nanodiamonds are the result of continuous rain, it would be expected that they should be present throughout the records, whereas they are almost absent outside the proposed boundary layer (15, 17).
v. If the evidence is not consistent with any of the possible extraterrestrial or impact origins, nanodiamonds must have originated from some kind of terrestrial process. It has been suggested that they might have formed during the wildfires responsible for the charred material in the YD boundary layer (46). Because wildfires are very common, this formation mechanism could also explain the age discrepancy. Artificial nanodiamonds have been grown using low-pressure CVD at temperatures as low as 450 °C (10, 11), although the ex-

perimental conditions differ from natural wildfire settings. Furthermore, particles with a cubic diamond structure as well as carbon onion structures, which can serve as nanoscopic pressure cells for diamond formation (49), have been observed in wood that was experimentally charred at 700 °C and subsequently cooled in a nitrogen atmosphere (50). In addition, cubic nanodiamonds (<5 nm) have recently been discovered in a candle flame and a natural gas flame (51). Although most nanodiamonds burn up in the flame, this discovery suggests it might be possible for nanodiamonds to form during a combustion-type process under normal atmospheric conditions. These findings are contrary to the suggestions of Kurbatov et al. (15) that nanodiamond formation requires extraordinary high temperature, pressure, and redox conditions not naturally found at the Earth's surface, leading them to adopt an extraterrestrial origin for the nanodiamonds in the Greenland ice sheet.

Although natural wildfires can reach temperatures as high as 900 °C, glass-like carbon and carbon spherules found in our study as well as the Black Mat (2, 6, 52) possibly indicate a low-temperature formation (<550 °C or more likely <400 °C; refs. 29 and 30). A wildfire temperature of approximately 420 °C, as inferred from our reflectance analysis at Geldrop-Aalsterhut, also indicates that temperatures were slightly too low for known diamond forming mechanisms. It must, however, be noted that the final reflectance value depends not only on temperature, but also on the duration of charring (22, 23). If heating occurred during a period of <1 h, the temperature would have been slightly higher then what we inferred from our reflectance values. For example, for a charring period of only 10 min, our value of 0.96% R_o would indicate a temperature of approximately 460 °C (22).

The carbon spherules found in the YD boundary layer seem similar to charred fungal sclerotia formed under relatively low temperatures (<450 °C; ref. 29). Although Daulton et al. (14) do not report any nanodiamonds in similar carbon spherules, cubic nanodiamonds have been found in carbon spherules from present-day forest soils (53). If the morphology of these carbon spherules to the charred fungal sclerotia is due to a similar low-temperature origin, this might suggest a yet unknown low-temperature formation of nanodiamonds. This similarity seems in agreement with our findings of nanodiamonds in glass-like carbon as well as the low wildfire temperature inferred from the charcoal. We cannot, however, exclude the possibility that the nanodiamonds were adhered to the surface of the glass-like carbon and might thus be unrelated.

In summary, although some formation scenarios seem less likely then others, the exact formation mechanism of the nano- and microdiamonds found in the YD boundary layer is still unknown. It is possible that several mechanisms have played a role. For example, a CVD-like process within an impact/airburst fireball or natural wildfire might have been responsible for the smaller rounded nanodiamonds reported (5, 6, 15, 16), although another process might be responsible for the larger flake-like and tabular nano- and microdiamonds (6, 16).

Finally, it must be noted that there is a wide range in diamond polymorphs and morphology reported from different locations and/or by different authors, which also seems the case for the diamonds reported at the K/T boundary (see Table S1). In addition, Daulton et al. (14) report that no nanodiamonds were present at all in their Black Mat samples, suggesting that differences in sample preparation, analysis and interpretation might also affect the results. In addition, sample size and relative abundances at different locations can be a problem. We analyzed several hundred particles in the TEM, representing only a fraction of the glass-like carbon in the samples, but only found less than a handful of possible nanodiamonds. We found no nanodiamonds in a small fraction of carbon spherules analyzed; this might, however, be related to the small sample size.

Conclusions

Our work follows two lines of research on the carbonaceous fraction of the Usselo horizon, associated with the proposed YD impact event. TEM analysis of glass-like carbon shows that, although cubic nanodiamonds are present, there is no sign of the shock polymorph lonsdaleite. Furthermore, although the formation of the Usselo horizon started during the Allerød, our critical dating places the wildfire episode up to two centuries after the proposed impact event and into the YD. Moreover, our nanodiamonds are two centuries younger then the diamonds reported by Kennett et al. (6), indicating that, unless two impacts happened in a short period of time, one or both of the cubic diamond populations must have a nonimpact origin. Because the glass-like carbon in which the nanodiamonds were found is known as a wildfire product, the nanodiamonds might in some way be related to wildfires instead. We therefore conclude that, although our findings cannot exclude the possibility of an impact, we found no evidence in the Usselo horizon to support the YD impact hypothesis.

Materials and Methods

Fieldwork. Samples were taken during one day of fieldwork at the archaeological site Geldrop-Aalsterhut. Several pits were manually dug using shovels and cleaned with trowels to locate the best part of the Usselo horizon to sample. Samples of 200–800 g of sediment were taken by the corresponding and second author from three selected locations in two pits at several intervals within and above the charcoal-rich part of the Usselo horizon (Fig. S1 and Table 1). One bulk sample of the charcoal layer at the top of the Usselo horizon at Aalsterhut, AH-4, was sampled by a colleague together with the second and last author during an earlier field visit.

Radiocarbon Dating. A total of 14 individual charcoal particles, >2 mm, from different samples (Table 1) were handpicked and prepared for AMS radiocarbon dating using standard acid-alkali-acid treatment and ultrasonic cleaning (54) by which only charcoal structures remained and soot disaggregated. Radiocarbon ages were measured at the Groningen AMS facility (55) and reported in conventional radiocarbon years (56). Ages were calibrated to calendar years using the IntCal09 calibration curve (34) and the OxCalv4.1 calibration software (27). Both the radiocarbon and calibrated ages are rounded to the nearest five; all uncertainties are given within 1-σ confidence.

Reflectance Analysis. Several charcoal particles, >2 mm, from sample AH-21 were embedded in resin blocks, polished, and submitted to reflectance analysis for a preliminary estimate of the wildfire temperature following the procedure described in ref. 22. For each particle, 100 measurements of the reflections were taken at different locations using a Leitz motorized digital microscope laboratory automatic microscope.

SEM Analysis. Subsamples of 100 g from samples AH-4, 14, and 33 were dried in the oven at 90 °C, and sieved into fractions of <63, 63–355, and >355 μm. The carbonaceous fraction of 63–355 μm was floated using sodiumpolytungstate heavy liquid with a density of 2,000 kg/m^3. Flotation in water, as used in the original study (2, 6), did not yield any carbon spherules. Carbon spherules and glass-like carbon were then picked under a light microscope (magnification 40×) based on their morphology (black spherical particles or black particles with an irregular shape and smooth, reflective glassy surface). The distinction between glass-like carbon and normal charcoal, however, was not always easy to make because there seems to be a gradual transition between the two with some charcoal particles having a partly glassy surface. Representative particles from samples AH-14 and 33 were mounted on a stub and analyzed using an FEI XL30SFEG SEM equipped with an EDAX energy-dispersive spectrometry (EDS) detector located at the Electron Microscopy Laboratory Utrecht (EMU).

TEM Analysis. Carbon spherules (sample AH-4) and glass-like carbon particles (samples AH-14 and 33) were separately grouped for TEM analysis. These were crushed in ethanol using an agate pestle and mortar, and part of the suspension dispersed on a holey carbon grid. TEM analysis was preformed using a FEI Tecnai 12 120 kV and a Tecnai 20 FEG 200 kV TEM equipped with an EDAX EDS detector, both located at EMU. The TEM grids were sampled

both in diffraction mode, to locate crystalline particles, and in image mode, to locate individual particles. In this way, several hundreds of particles per grid were analyzed. Selected area diffraction patterns were used to identify the crystal structure of the particles, and energy dispersive X-ray spectrometry was used to check the carbon content.

ACKNOWLEDGMENTS. We thank Jos Deeben (Rijksdienst voor het Cultureel Erfgoed) for access to the field site; Maartje Hamers (Utrecht University) for taking samples during an earlier fieldwork; Hans Meeldijk and Tilly Bouten (Utrecht University) for help with the EM work; and Deltares (Utrecht) for the use of their equipment and technical assistance with the reflectance measurements.

1. Fiedel SJ (2011) The mysterious onset of the Younger Dryas. *Quat Int* 242:262–266.
2. Firestone RB, et al. (2007) Evidence for an extraterrestrial impact 12,900 years ago that contributed to the megafaunal extinctions and the Younger Dryas cooling. *Proc Natl Acad Sci USA* 104:16016–16021.
3. Pinter N, et al. (2011) The Younger Dryas impact hypothesis: A requiem. *Earth Sci Rev* 106:247–264.
4. Kerr RA (2008) Paleontology: Experts find no evidence for a mammoth-killer impact. *Science* 319:1331–1332.
5. Kennett DJ, et al. (2009) Nanodiamonds in the Younger Dryas boundary sediment layer. *Science* 323:94.
6. Kennett DJ, et al. (2009) Shock-synthesized hexagonal diamonds in Younger Dryas boundary sediments. *Proc Natl Acad Sci USA* 106:12623–12628.
7. Hanneman RE, Strong HM, Bundy FP (1967) Hexagonal diamonds in meteorites: Implications. *Science* 155:995–997.
8. Masaitis VL (1998) Popigai crater: Origin and distribution of diamond-bearing impactites. *Meteorit Planet Sci* 33:349–359.
9. Gilmour I (1998) Geochemistry of carbon in terrestrial impact processes. *Geol Soc Spec Publ* 140:205–216.
10. Frenklach M, et al. (1989) Homogeneous nucleation of diamond powder in the gas phase. *J Appl Phys* 66:395–399.
11. Daulton TL, Eisenhour DD, Bernatowicz TJ, Lewis RS, Buseck PR (1996) Genesis of presolar diamonds: Comparative high-resolution transmission electron microscopy study of meteoritic and terrestrial nano-diamonds. *Geochim Cosmochim Acta* 60:4853–4872.
12. Koeberl C, et al. (1997) Diamonds from the Popigai impact structure, Russia. *Geology* 25:967–970.
13. French BM, Koeberl C (2010) The convincing identification of terrestrial meteorite impact structures: What works, what doesn't, and why. *Earth Sci Rev* 98:123–170.
14. Daulton TL, Pinter N, Scott AC (2010) No evidence of nanodiamonds in Younger-Dryas sediments to support an impact event. *Proc Natl Acad Sci USA* 107:16043–16047.
15. Kurbatov AV, et al. (2010) Discovery of a nanodiamond-rich layer in the Greenland ice sheet. *J Glaciol* 56:747–757.
16. Tian H, Schryvers D, Claeys P (2011) Nanodiamonds do not provide unique evidence for a Younger Dryas impact. *Proc Natl Acad Sci USA* 108:40–44.
17. Israde-Alcántara I, et al. (2012) Evidence from central Mexico supporting the Younger Dryas extraterrestrial impact hypothesis. *Proc Natl Acad Sci USA* 109:E738–E747.
18. Israde-Alcántara I, et al. (2010) Paleolimnologic evolution of Lake Cuitzeo, Michoacán, during the Pleistocene-Holocene (Translated from Spanish). *Bol Soc Geol Mex* 62:345–357.
19. Kaiser K, et al. (2009) Palaeopedological marker horizons in northern central Europe: Characteristics of Lateglacial Usselo and Finow soils. *Boreas* 38:591–609.
20. Kasse C (2002) Sandy aeolian deposits and environments and their relation to climate during the Last Glacial Maximum and Lateglacial in northwest and central Europe. *Prog Phys Geog* 26:507–532.
21. De Vries H, Barendsen GW, Waterbolk HT (1958) Groningen radiocarbon dates II. *Science* 127:129–137.
22. Braadbaart F, Poole I (2008) Morphological, chemical and physical changes during charcoalification of wood and its relevance to archaeological contexts. *J Archaeol Sci* 35:2434–2445.
23. McParland LC, Collinson ME, Scott AC, Campbell G (2009) The use of reflectance values for the interpretation of natural and anthropogenic charcoal assemblages. *Archaeol Anthropol Sci* 1:249–261.
24. Vermeersch PM (2011) The human occupation of the Benelux during the Younger Dryas. *Quat Int* 242:267–276.
25. De Bie M, Vermeersch PM (1998) Pleistocene-holocene transition in Benelux. *Quat Int* 49-50:29–43.
26. Riede F (2008) The laacher see-eruption (12,920 BP) and material culture change at the end of the Allerød in northern Europe. *J Archaeol Sci* 35:591–599.
27. Bronk Ramsey C (2009) Bayesian analysis of radiocarbon dates. *Radiocarbon* 51:337–360.
28. Haynes CV, Jr (2008) Younger Dryas "Black Mats" and the Rancholabrean termination in North America. *Proc Natl Acad Sci USA* 105:6520–6525.
29. Scott AC, et al. (2010) Fungus, not comet or catastrophe, accounts for carbonaceous spherules in the Younger Dryas "impact layer". *Geophys Res Lett* 37:L14302.
30. McParland LC, Collinson ME, Scott AC, Campbell G, Veal R (2010) Is vitrification in charcoal a result of high temperature burning of wood? *J Archaeol Sci* 37:2679–2687.
31. Edington JW (1975) *Electron Diffraction in the Electron Microscope* (Phillips, Eindhoven, The Netherlands), p 100.
32. Gavin DG (2001) Estimation of inbuilt age in radiocarbon ages of soil charcoal for fire history studies. *Radiocarbon* 43:27–44.
33. Hoek WZ, Bohncke SJP (2002) Climatic and environmental events over the Last Termination, as recorded in The Netherlands: A review. *Neth J Geosci* 81:123–137.
34. Reimer PJ, et al. (2009) IntCal09 and Marine09 radiocarbon age calibration curves, 0–50,000 years CAL BP. *Radiocarbon* 51:1111–1150.
35. Blockley SPE, et al. (2012) Synchronisation of palaeoenvironmental records over the last 60,000 years, and an extended INTIMATE event stratigraphy to 48,000 b2k. *Quat Sci Rev* 36:2–10.
36. Mangerud J, Andersen ST, Berglund BE, Donner JJ (1974) Quaternary stratigraphy of Norden, a proposal for terminology and classification. *Boreas* 3:109–128.
37. Goslar T, et al. (1995) High concentration of atmospheric 14C during the Younger Dryas cold episode. *Nature* 377:414–417.
38. Hajdas I, Bonani G, Bodén P, Peteet DM, Mann DH (1998) Cold reversal on Kodiak Island, Alaska, correlated with the European Younger Dryas by using variations of atmospheric 14C content. *Geology* 26:1047–1050.
39. Kaiser KF, et al. (2012) Challenging process to make the Lateglacial tree-ring chronologies from Europe absolute—an inventory. *Quat Sci Rev* 36:78–90.
40. Rasmussen SO, et al. (2006) A new Greenland ice core chronology for the Last Glacial Termination. *J Geophys Res* 111:1–16.
41. Hoek WZ (1997) Late-glacial and early Holocene climatic events and chronology of vegetation development in The Netherlands. *Veg Hist Archaeobot* 6:197–213.
42. van der Hammen T, van Geel B (2008) Charcoal in soils of the Allerød-Younger Dryas transition were the result of natural fires and not necessarily the effect of an extraterrestrial impact. *Neth J Geosci* 87:359–361.
43. Marlon JR, et al. (2009) Wildfire responses to abrupt climate change in North America. *Proc Natl Acad Sci USA* 106:2519–2524.
44. Gill JL, Williams JW, Jackson ST, Lininger KB, Robinson GS (2009) Pleistocene megafaunal collapse, novel plant communities, and enhanced fire regimes in North America. *Science* 326:1100–1103.
45. Haynes CV, et al. (2010) The Murray Springs Clovis site, Pleistocene extinction, and the question of extraterrestrial impact. *Proc Natl Acad Sci USA* 107:4010–4015.
46. Paquay FS, et al. (2009) Absence of geochemical evidence for an impact event at the Bølling-Allerød/Younger Dryas transition. *Proc Natl Acad Sci USA* 106:21505–21510.
47. Hough RM, Gilmour I, Pillinger CT, Langenhorst F, Montanari A (1997) Diamonds from the iridium-rich K-T boundary layer at Arroyo el Mimbral, Tamaulipas, Mexico. *Geology* 25:1019–1022.
48. Dai ZR, et al. (2002) Possible in situ formation of meteoritic nanodiamonds in the early solar system. *Nature* 418:157–159.
49. Banhart F, Ajayan PM (1996) Carbon onions as nanoscopic pressure cells for diamond formation. *Nature* 382:433–435.
50. Ishimaru K, et al. (2001) Diamond and pore structure observed in wood charcoal. *J Wood Sci* 47:414–416.
51. Su Z, Zhou W, Zhang Y (2011) New insight into the soot nanoparticles in a candle flame. *Chem Commun* 47:4700–4702.
52. Kennett DJ, et al. (2008) Wildfire and abrupt ecosystem disruption on california's northern channel islands at the Allerød-Younger Dryas boundary (13.0-12.9 ka). *Quat Sci Rev* 27:2530–2545.
53. Yang ZQ, et al. (2008) TEM and Raman characterisation of diamond micro- and nanostructures in carbon spherules from upper soils. *Diamond Relat Mater* 17:937–943.
54. Mook WG, Streurman HJ (1983) Physical and chemical aspects of radiocarbon dating. *PACT* 8:31–55.
55. van der Plicht J, Wijma A, Aerts AT, Pertuisot MHP, Meijer HAJ (2000) The Groningen AMS facility: Status report. *Nucl Instrum Methods Phys Res B* 172:58–65.
56. Mook WG, van der Plicht J (1999) Reporting ^{14}C activities and concentrations. *Radiocarbon* 41:227–239.

Supporting Information

van Hoesel et al. 10.1073/pnas.1120950109

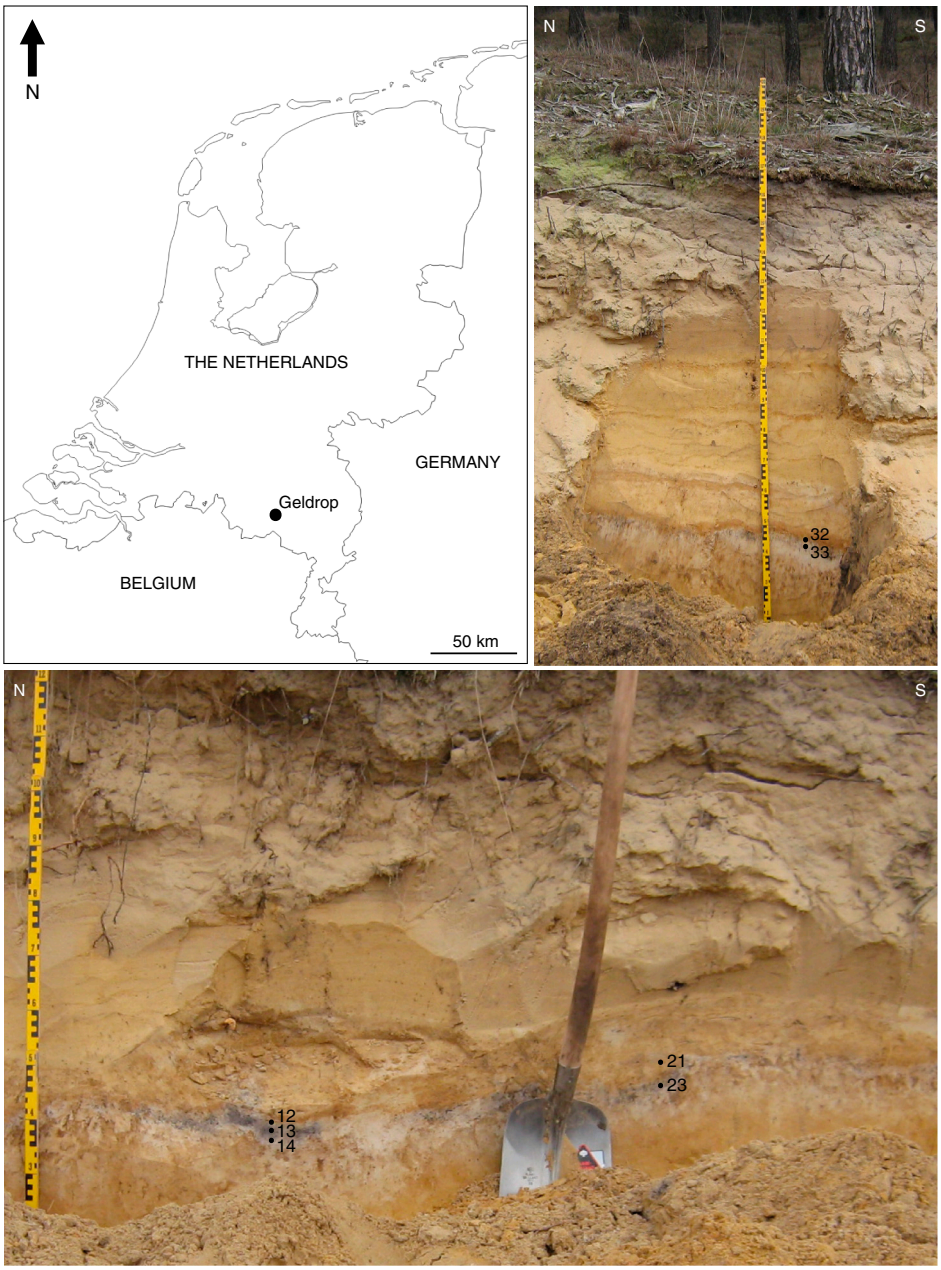

Fig. S1. Location of the field site (Geldrop-Aalsterhut) and the charcoal samples from the Usselo Horizon used for ^{14}C dating. The section shown at the top is located approximately 20-m south of the section shown at the bottom. See Fig. 1 for stratigraphy and Table 1 for specific depth of the samples.

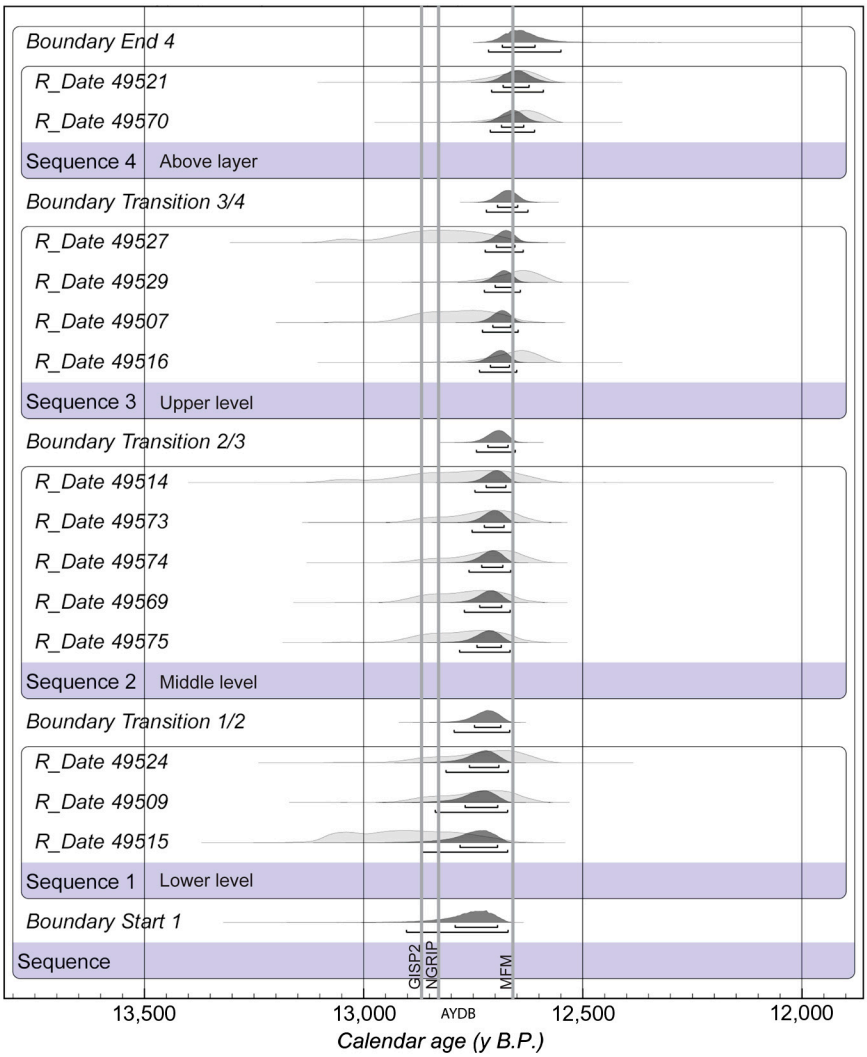

Fig. S2. Modeled (dark gray) and unmodeled (light gray) calibrated age of the charcoal particles in calendar years B.P. Bayesian analysis was performed using the OxCal v4.1.7 program (1). Dates were grouped according to their respective location within the charcoal-rich part of the Usselo horizon (see also Table 1 and Fig. S1), boundaries between the levels are calculated by the model. The distribution of the modeled dates is much narrower then the single calibrated ages. Although the modeled dates show a trend toward younger dates at the top, they all overlap within two standard deviations. Furthermore, the boundaries between the different groups all overlap within one standard deviation, making them statistically the same. The Allerød-Younger Dryas boundary (AYDB) is indicated according to the Greenland Ice Sheet Project 2 and North Greenland Ice Core Project ice cores (2, 3) as well as the Meerfelder Maar (MFM) varved lake. The timing of the onset of the Younger Dryas as derived from the ice cores most likely represent the timing of the alleged impact because the Greenland ice sheet would have recorded the destabilization of the thermohaline circulation to which the impact has been linked by Firestone et al. (4).

1 Bronk C (2009) Bayesian analysis of radiocarbon dates. *Radiocarbon* 51:337–360.
2 Stuiver M, Grootes PM, Braziunas TF (1995) The GISP2 δ18O climate record of the past 16,500 years and the role of the sun, ocean, and volcanoes. *Quat Res* 44:341–354.
3 Rasmussen SO, et al. (2006) A new Greenland ice core chronology for the last glacial termination. *J Geophys Res* 111:1–16.
4 Firestone RB, et al. (2007) Evidence for an extraterrestrial impact 12,900 years ago that contributed to the megafaunal extinctions and the Younger Dryas cooling. *Proc Natl Acad Sci USA* 104:16016–16021.

Table S1. Overview of different diamond polymorphs and morphologies as found within the Allerød-Younger Dryas boundary as reported by different researchers

		Cubic diamond							n-diamond	Lonsdaleite (2H diamond)		
						Polycrystalline						
		Octahedral nano	Rounded nano	Flakes micro	Irregular shape	Hexagonal	Rectangular	Irregular	Rounded nano	Rounded nano	Tabular nano	tabular micro
Younger Dryas boundary												
	Kennett et al. (1) carbon spherules bulk sediment		X						X			
	Kennett et al. (2) carbon spherules carbon elongates				X				X			X*
	Daulton et al. (3) carbon spherules glassy carboncharcoal											
	Kurbatov et al. (4) ice sheet[†]								X	X[‡]	X[‡]	
	Tian et al. (5) bulk black material		X	X								
	Israde-AlcÆntara et al. (6) bulk sediment		~						X	X		
	This study, glass-like carbon							X				
Other												
	K/T boundary[§]	X			X	X	X					
	Recent C spherules Yang et al. (7)		X	X								

Results from the Cretaceous/Tertiar boundary nanodiamonds and recent carbon spherules have been added for comparison. K/T, Cretaceous/Tertiar.

*Misses the 1.93 and 1.5 reflections typical for lonsdaleite. Daulton et al. (3) suggested these are actually graphene/graphane aggregates misinterpreted as lonsdaleite.

[†]Ice layer not dated with absolute certainty. Pinter et al (8) argue that the oxygen isotopes suggested a Holocene age rather then Late Glacial.

[‡]Kurbatov et al. (4) claim that the nanodiamonds they found are "morphological and analytically indistinguishable from the lonsdaleite and n-diamonds found across North America in YDB carbon spherules and sediments." Rounded or nanosized tabular lonsdaleite is however not reported by Kennett et al. (1, 2)

[§]Carlisle and Bramant (9), Gilmour et al (10), and Hough et al (11).

1 Kennett DJ, et al (2009) Nanodiamonds in the Younger Dryas boundary sediment layer. *Science* 323:94.
2 Kennett DJ, et al (2009) Shock-synthesized hexagonal diamonds in Younger Dryas boundary sediments. *Proc Natl Acad Sci USA* 106:12623–12628.
3 Daulton TL, Pinter N, Scott AC (2010) No evidence of nanodiamonds in Younger-Dryas sediments to support an impact event. *Proc Natl Acad Sci USA* 107:16043–16047.
4 Kurbatov AV, et al. (2010) Discovery of a nanodiamond-rich layer in the Greenland ice sheet. *J Glaciol* 56:747–757.
5 Tian H, Schryvers D, Claeys P (2011) Nanodiamonds do not provide unique evidence for a Younger Dryas impact. *Proc Natl Acad Sci USA* 108:40–44.
6 Israde-Alcántara I, et al. (2012) Evidence from central Mexico supporting the Younger Dryas extraterrestrial impact hypothesis. *Proc Natl Acad Sci USA* 109:E738–E747.
7 Yang ZQ, et al. (2008) TEM and Raman characterisation of diamond micro- and nanostructures in carbon spherules from upper soils. *Diamond Relat Mater* 17:937–943.
8 Pinter N, et al. (2011) The Younger Dryas impact hypothesis: A requiem. *Earth Sci Rev* 106:247–264.
9 Carlisle DB, Braman DR (1991) Nanometre-size diamonds in the Cretaceous/Tertiary boundary clay of Alberta. *Nature* 352:708–709.
10 Gilmour I, et al. (1992) Terrestrial carbon and nitrogen isotopic ratios from cretaceous-tertiary boundary nanodiamonds. *Science* 258:1624–1626.
11 Hough RM, Gilmour I, Pillinger CT, Langenhorst F, Montanari A (1997) Diamonds from the iridium-rich K-T boundary layer at Arroyo el Mimbral, Tamaulipas, Mexico. *Geology* 25:1019–1022.